Osuani F. Idema[1,2], Malik Abdulwahab[1,3], Innocent O. Arukalam[1,4], Ifeyinwa C. Ekeke[1,5], Chigoziri N. Njoku[1,5], Anyiam N. Chioma[1,6], Ikenna B. Onyeachu[1,7], Emeka E. Oguzie[1]*

[1]Africa Centre of Excellence in Future Energies and Electrochemical Systems ACE-FUELS, Federal University of Technology, Owerri, Imo State, Nigeria, [2] Federal Polytechnic of Oil and Gas, Bonny, Rivers state, Nigeria [3.]Department of Metallurgical and Materials Engineering, Air Force Institute of Technology, Kaduna, Nigeria, [4]Department of Polymer and Textile Engineering, Federal University of Technology, Owerri, Imo State, Nigeria, [5]Department of Chemical Engineering, Federal University of Technology, Owerri, Imo State, Nigeria, [6]Department of Prosthetics and Orthotics, School of Health Technology, Federal University of Technology, Owerri, Imo State, Nigeria, [7]College of Science and Computer, Wigwe University Isiokpo, Rivers State, Nigeria.

Scientific paper
ISSN 0351-9465, E-ISSN 2466-2585
https://doi.org/10.62638/ZasMat1580

Zastita Materijala 67 ()
(2026)

Effectivness of *Musa Paradisiaca Leaves* (MPL) extract for carbon steel corrosion protection in sea water

ABSTRACT

The effectiveness of Musa Paradisiaca Leaf (MPL) extract-based corrosion inhibitor for carbon steel in 3.5wt.% NaCl solution has been studied using Fourier Transform Infrared Spectroscopy(FT-IR), Gravimetric Method (GM), Potentiodynamic Polarization (PDP) and Electrochemical Impedance Spectroscopy (EIS), Contact angle measurement (Θ), Density Functional Theory(DFT) and Molecular Dynamics(MD) simulations. The FTIR analysis showed presence of polar functional groups. While the GM revealed inhibition efficiency of 91% and a reduced corrosion rate from 0.8817 to 0.0823 mm/y. Likewise, PDP via Tafel plots showed a cathodic slope capable of controlling both activation (oxidation) and diffusion (oxygen reduction) reactions, indicating a mixed-type inhibitor, also the concentration of MPL extract at 100g/L showed a corrosion rate of about 0.1mm/y with an efficiency of 90.1%. EIS via Nyquist plot showed a semicircle with widened diameter and increased peak heights indicating a higher charge transfer resistance (R_{ct}). Contact angle measurements showed presence of thin films on the metal/inhibitor interface. Further, DFT analysis showed the presence of electron-rich centers, heteroatoms, polar functional groups which correlated the results by affirming the contributions of the isolated compounds of the MPL inhibitor molecule to the high inhibition efficiency. In addition, MD simulation showed presence of Langmuir films on the inhibitor/metal interface in planer orientation and large surface coverage. Radial distribution function (RDF) showed presence of short bond lengths of between 2.97Å-3.49Å, confirming the presence of chemical bonding. These highlights suggest that the corrosion inhibition performance of MPL is like that of a typical surfactant and attributed this to the presence of saponins in its molecule.

***Keywords**: Carbon steel corrosion, Contact angle measurement, DFT&MD simulation, electrochemical measurement, gravimetric analysis, Musa ParadisiacaLeaves, Surfactant*

1. INTRODUCTION

Generally speaking, steel is one of the widely used materials for the construction of a wide range of infrastructures. However, unlike other metals and alloys whose corrosion products form a natural protective outer layer when exposed to the environment, steel doesn't, especially in chloride environment. As a result, steel and its alloys as well as other metals are susceptible to corrosion.

*Corresponding author: Osuani F. Idema
E-mail**:** idema.o@acefuels-futo.org
Paper received: 14. 09. 2025.
Paper corrected: 13. 05. 2026.
Paper accepted: 14. 05. 202.6

Corrosion can be referred to as the deterioration, degradation and loss of a material and its critical properties due to interaction with its environment. It can also be saidto be the oxidation that occurs on a metal when exposed to its immediate environment.

Similarly, corrosion can originate when a metal reacts with oxygen, hydrogen, electrical current, dirt, or even bacteria. Corrosion causes the deterioration of infrastructure and it can lead to unexpected failures, loss of lives and productive hours.

Because of the debilitating effects of corrosion, the attendant economic cost is huge. According to

the National Association of Corrosion Engineers (NACE), the estimated annual cost of corrosion is at $2.5 trillion. This represents 3% of the global gross domestic product (GDP) [1,2]. Therefore, it makes economic sense to prevent, control or mitigate the corrosion menace.

In fact, NACE has estimated that implementing best practices in corrosion prevention could result to as much as $875 billion in savings [2]. To achieve this, the methods to adopt in corrosion mitigation and control could include the following: (a) selection of materials (b) application of corrosion inhibitors (c) application of coatings (d) cathodic protection and (e) design.

Considering the above methods, the application of corrosion inhibitors especially plant extracts, will form the focus of this paper since they are environment-friendly. The application of these eco-friendly inhibitors including ionic liquids [3] which aligns with the growing emphasis on sustainability in industrial practices, offering a promising opportunity for corrosion management without compromising environmental and health standards.

Plant extracts are considered to be an abundant source of naturally derived chemical substances that can be extracted from various parts of plants, such as leaves, stem, root, bark, fruits, fruit peel, seeds, flowers, husks, and nuts, which contain phytochemicals like alkaloids, flavonoids, heteroatoms, tannins, saponins and nitrogen-based compounds. They are easily extracted and inexpensive.

Also, they are naturally abundant and biodegradable[4-6]. These benefits explain why plant extracts and their byproducts are employed as organic corrosion inhibitors for the mitigation, control and management of corrosion in various environments. Plant extracts are rich in polar molecules with oxygen, O; nitrogen, N; sulfur, S as well as non-polar compounds with aromatic rings, aliphatic chains, heterocyclic rings, and functional moieties[7]. Certainly, these have been reported to promote the interfacial adsorption of inhibitors on the surfaces of metals by forming a protective thin film on metallic surfaces without affecting the surroundings and hence decrease the corrosion rate[4,8,9]. It involves the removal of water molecules and formation of a protective thin film on the surface of the substrate. This adsorption can be describedas chemisorption based on whether the compound forms robust, ionic or covalent bonds on the surface of thesubstrateor as physisorption if onlyvan der Waals force of electrostatic interactions occurred. In other to effectively extract these organic or plant extracts, methanol, ethanol, acetone or an aqueous solvent is used.However, the use of plant extracts as inhibitors of corrosion was introduced in1930 when extracts from *Chelidoniummajus* and some other plants were first applied in sulfuric acid, H_2SO_4 medium [10, 11]. Subsequently,there has been enormous report on the use of plant extracts for corrosion control. In view of this, Wang et al. [12] evaluated *Ficus tikoua* leaves for carbon steel corrosion in 1.MHCl using PDP, EIS, DFT, MD, AFM, SEM and reported an inhibition efficiency of up to 95.8% at 298K. While Chen et al.[13] investigated *Magnolia grandiflora* leaves for corrosion inhibition of Q235 steel in 1MHCl using DFT, MD, AFM, and SEM, and reported an inhibition efficiency of 85% at 298K functioning as a mixed-type inhibitor. Also, Carmona-Hernandez et al.[14] evaluated *Pistia stratiotes* leaf as green corrosion inhibitor for mild steel in 1MHCl using EIS, PDP, SEM, EDS, GC-MS and reported an inhibition efficiency of 93.7% functioning as a mixed-type inhibitor. Sabiha et al.[15] investigated the adsorption and corrosion inhibition efficacy and mechanism of *Marjoram* leaves extract on mild steel in 1MHCl using PDP, EIS, WL, SEM, EDX and reported an inhibition efficiency of up to 87.1% functioning as a mixed-type inhibitor. Elyoussfi et al.[16] investigated the anticorrosion properties of *Origanum grossi* extract for mild steel corrosion in 1MHCl using EIS, PDP, WL, SEM,/EDX, DFT, MD and reported an inhibition efficiency of 92% while functioning as a mixed-type inhibitor. Haddou et al.[17] evaluated *Cannabis sativa* L. extract as corrosion inhibitor for mild steel in 1MHCl using WL, EIS, PDP, DFT, MD and reported an inhibition efficiency of between 83-91% while acting as a mixed-inhibitor. Tabyaoui et al.[18] evaluated the inhibition properties of *Citrullus colocynthis* in 1MHCl using GM, PDP, AC impedance, SEM, FT-IR, XPS, DFT, MD and reported aninhibition efficiency of 93.6% acting as a mixed-type inhibitor. Nadi et al.[19] studied the inhibition effect of *Sargassum muticum* extract in 1MHCl using GM, electrochemical technique, XPS and reported an inhibition efficiency of 97% acting as a mixed-type inhibitor for carbon steel. Dent and Fuchs-Godec.[20] evaluated the inhibitory activity of *Salvia officialis L*. in 3.0%NaCl using EIS, PDP, ATR-FTIR and reported impressive inhibition efficiency of 94.1%. Cojocaru et al.[21] on their part investigated *Galium verum* plant extract for steel corrosion protection in 1MHCl using PDP, EIS, HPLC, GC-MS and reported an inhibition efficiency of 91.82%. Mohamed et al.[22] evaluated *Inula viscosa* root extract as a potent corrosion inhibitor for mild steel in 1MHCl using EIS, PDP, SEM, high performance liquid chromatography and reported an inhibition efficiency of up to 97.7%. Akalezi et al.[23] investigated the corrosion inhibition properties of *Moringa oleifera* on mild steel in

0.5MH_2SO_4 using weight Loss, PDP, EIS, SEM, DFT and reported an inhibition efficiency of 93.0% while also acting as a mixed type corrosion inhibitor.

In this paper *Musa paradisiaca* plant leaves has been chosen for evaluation. It is a perennial plant that grows on the tropical and subtropical regions of the world and it is cultivated for its nutritional and medicinal benefits. Due to its huge traditional value, researchers are actively studying its bioactive metabolites and pharmacological applications to a large extent. A comprehensive literature search revealed that the plant contains phytochemicals such as alkaloids, glycosides, saponins, tannins, flavonoids, terpenoids and steroids[24-30]. In a particular study, Adeolu and Enesi.[31] studied the phytochemical constituents of Musa paradisiaca using standard methods of analyses of Association Official Analytical Chemists and Atomic Adsorption Spectrophotometric method. The phytochemical results revealed the presence of bioactive compounds such as; alkaloids (24mg/100g), tannins (115mg/100g), flavonoids (145mg/100g), phenols (4.5mg/100g), saponins (563.33mg/100g), phytates (46.67 mg/100g) and oxalates (30mg/100g). In another study, Ekeke et al [32] investigated the efficacy of Musa paradisiaca stem sap extract on aluminum corrosion in acidic environment using GC-MS, EIS, AFM and achieved an inhibition efficiency of 90.73%. It is very clear from the literature that the use of plant extracts in corrosion mitigation is gaining prominence as their use has been successful without polluting the environment [33-36]

Theaim of this paper is toevaluate the effectiveness of *Musa Paradisiaca* Leaf (MPL) extract for carbon steel corrosion protection in 3.5wt% NaCl. To achieve this aim, the specific objectives are to: determine the presence of polar functional groups in the MPL molecule usingFourier transform infrared spectroscopy (FT-IR); determine weight loss, corrosion rate and inhibiton efficiency using gravimetric method;determine reaction rates, current density/corrosion rate using potentio-dynamic polarization (PDP);determine charge transfer resistance/polarization resistance using electrochemical impedance spectroscopy (EIS);determine surface interaction using contact angle measurements (Ɵ),determine global descriptors for molecular level interaction using density functional theory (DFT)and molecular dynamics (MD) simulation.In order to carry out the DFT calculations and MD modeling and/ simulations, some notable compounds present in the MPL molecule as reported elsewhere [37]such as; M1=6-Amino-1,3,5-triazine-2,4(1H,3H)-dione; M2=2,3-Dihydrothiaphene; M3= 2-Deoxyhexopyra-nose; M4=Octamethylcyclotetrasilozane; M5= 2,6,10-Dodecatrien-1-ol,3,7,11-trimethyl-(2Z,6Z); M6=9-Octadecenamide were chosen. Where, “M” represents each of the compounds. Figure 1 shows their chemical structures and formulae

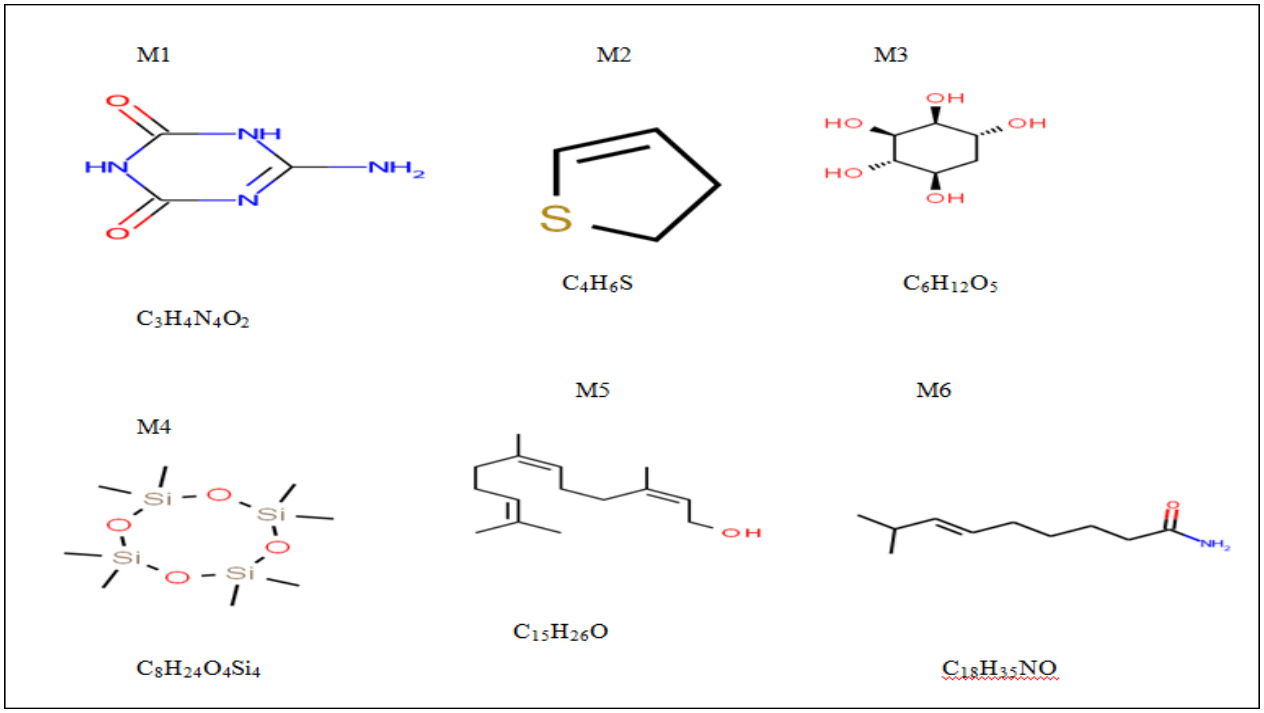

Figure 1. Shows chemical structures and formulae of some notable compounds present in MPL molecule [37]

2. EXPERIMENTALS

2.1. Preparation of metal Specimen

Carbon steel (substrate) specimen was selected for this study.It is an iron-carbon alloy of density 7.85g/cm^{3}and other trace elements. The chemical composition and steel grade is shown in table1.

Table 1. Chemical composition and grade of test specimen

Material	Elemental Composition (wt. %)									
ASTM A106 Grade B	C	Mn	P	S	Mo	Si	Ni	Cr	Cu	V
	0.3	1.06	0.035	0.035	0.15	0.10	0.4	0.4	0.4	0.08

The preparation of test specimen followed ISO 11845 standard procedure. The original material was a pipe and cut into sizes of 2.0 cm x 2.0 cm x 0.6 cm dimensions for the test, a wire brush was used to de-scale it. Thereafter, the coupons were placed on the metallographic lapping and polishing machine (UNIPOL-820) manufactured by Zhengzhou CY Scientific Instrument Co., Ltd, where they were neatly polished using abrasive emery paper of grit sizes of between150 and 1000 micron of various grades. This was done to obtain a very smooth surface for the weight loss measurements. In course of the machining, attention was given to the edges for proper polishing. Furthermore, the coupons were washed with distilled water, degreased in ethanol, dry cleaned and dipped into acetone. Then, they were dried with dry air and stored under a desicator containing silica gel until when they were used.

2.2. Preparation of MPL extract

The MPL was collected at Port Harcourt, Rivers State, Nigeria. They were then transported in a clean sack bag to the Africa Centre of Excellence in Future Energies and Electrochemical Systems General Purpose Research Laboratory at Federal University of Technology, Owerri, where the leaves were oven dried before crushing into powdered form. Thereafter, it was then weighed, dissolved into 70% ethanol and then allowed to stay for 48 hours before it was extracted and concentrations of 10g/L, 20g/L, 40g/L, 60g/L, 80g/L and 100g/L prepared from it and stored for use according to Verma et al (https://creativecommons.org/ licenses/ by-nc/3.0/) [1] as shown in figure 2.

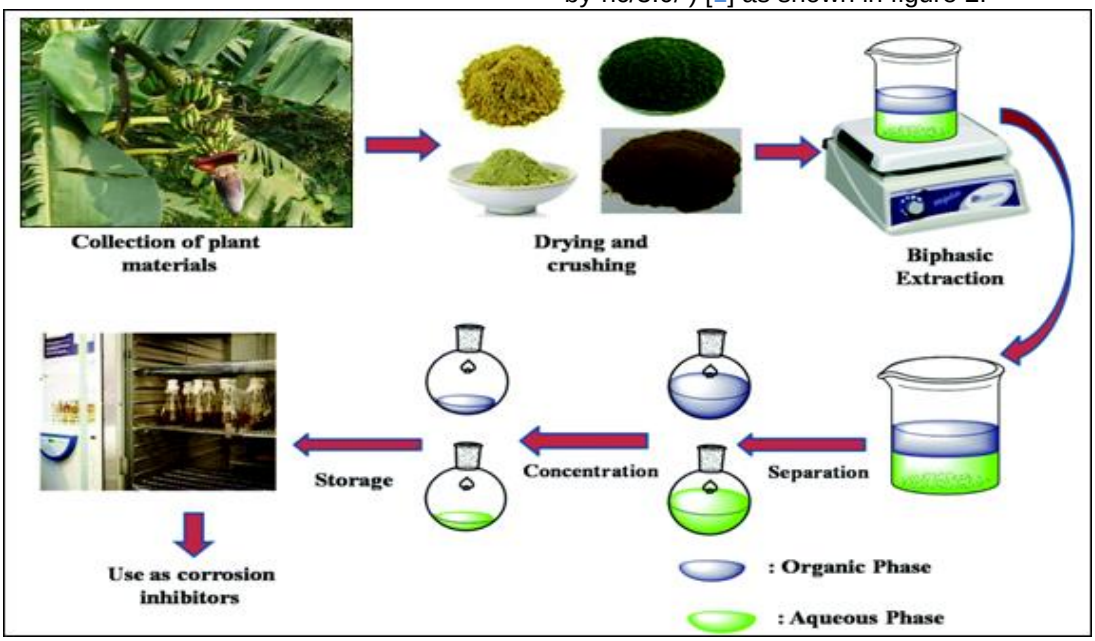

Figure 2. Inhibitor Preparation Process [1]

2.3. Preparation/Simulation of seawater(3.5wt % NaCl)test solution

The test solution was prepared by measuring 35g of NaCl and dissolving it into 1litre of de-

ionized water to have 3.5wt%NaCl solution. After then, the various MPL inhibitor concentrations were mixed with the test solution in different beakers for immersion.

2.4. Fourier Transform Infrared Spectroscopy (FT-IR) Analysis

Perkin Elmer spectrum 2 (UATR) FT-IR, IR 10.7.2 was used to carry out the FT-IR analysis on the MPL extract to evaluate the types of functional groups present. A liquid sample of the MPL extract was used. Firstly, the liquid cell of the FT-IR was assembled with the IR transparent window. And then, a few drops of the liquid sample was introduced into the cell and carefully sealed. Secondly, the sample was placed in the FT-IR spectrometer and scanned. The spectrometer directs infrared beams at the sample and the absorbance is measured taking the frequency into consideration. Finally, the spectrum is then analyzed and the details of analysis shown in figure 4 and table 2.

2.5. Gravimetric or Weight Loss Measurement

The polished and pre-weighed carbon steel specimens were immersed in the 3.5% NaCl solution containing the MPL inhibitor in concentrations of 10g/L, 20g/L, 40g/L, 60g/L, 80g/L and 100g/L for exposure times of 1h, 6h, 24h, 48h, 72h, 96h and 120h at constant temperature of 298k. After the exposure period, the specimens were carefully removed from the solution and put into a stainless steel container containing detergent and left for a few seconds. Firstly, the specimens were thoroughly washed in the detergent using a strong plastic bristle brush adopting consistent scrubbing, scraping and brushing. Next, chemical cleaning was introduced using reagent grade chemical (acetone) by dipping the cleaned specimens inside the chemical to get rid of any resin or contaminant on the surface of the specimen, they were then hot dried using a hand drier. Thereafter, the weights were measured and the weight loss recorded in triplicate. Results were reported in average values ± SD (standard deviation). To ensure accuracy and reproducibility of the results, the XINGYUN FA2104 Electronic weighing balance with reading accuracy of 0.0001g and linearity error of 0.0003g was used. The obtained weight loss results were used to calculate the carbon steel corrosion rate in the presence and absence of the MPL extract-based inhibitor and their inhibition efficiencies using Eq.1:

Weight Loss,

$$\Delta W = W_i - W_f \qquad (1)$$

Where, ΔW is weight loss, W_i is the initial weight before immersion, W_f is the final weight after immersion.

The corrosion rate was calculated using Eq. 2. [11]:

Corrosion Rate,

$$CR\ (mm/y) = [\Delta W \times \kappa]/ \rho\, AT \qquad (2)$$

Where K = 87600, ΔW is weight loss (g), ρ is density (g/cm^3), A is the surface area of the Specimen (cm^2) and T is the exposure time in hours [11].

The inhibition efficiency (%IE) was calculated using Eq.3:

$$\%IE = [(CR_A - CR_P) / CR_A] \times 100 \qquad (3)$$

Where, CR_A and CR_P are the corrosion rates in the absence and presence of the MPL inhibitorrespectively.

Also, the maximum saturation surface occupied of the inhibitor on a given available adsorption surface known as the surface coverage is determined using the Eq. 4:

Surface Coverage

$$(\theta) = Inhibition Efficiency,\ IE \div 100 \qquad (4)$$

2.6. Electrochemical Investigation of MPL on carbon steel in 3.5wt% NaCl

Samples for the electrochemical investigation were test coupons of 1.0cm x 1.0 cm^2. The Electrochemical investigations were carried out using a Radiometer analytical PGZ100 potentiostat device, controlled by a computer equipped with Volta master 4 software, which allows data acquisition and processing. For electrochemical tests, a conventional three electrode cell was used: A saturated calomel electrode (SCE) reference electrode, a platinum counter electrode, and a carbon steel working electrode. Before each experiment, the working electrode is kept immersed for 30 minutes at the open circuit potential (OCP), this appropriate time is necessary to obtain the stabilization of the free potential (EOCP). Electrochemical impedance spectroscopy measurements were carried out at the open circuit potential with an applied frequency starting from 100 kHz at 0.01 Hz using sinusoidal potential perturbation. The Nyquist representations of the impedance were analyzed and simulated by EC-Lab software, and then the EIS parameters were determined. The polarization curves were obtained with a scan rate of 1mV.s^{-1} and in the potential range −1800 to −600 mV/SCE in the presence of MPL inhibitor at different concentrations after EIS measurements were taken considering the equivalent circuit in figure 3. The inhibition

efficiency IE_{EIS} (%) and IE_I (%) was calculated by Eqs. 5 and 6:

$$IE_{EIS}\,(\%) = (1 - R_P/R_{PO}) \times 100 \quad (5)$$

Where, IE_{EIS} = inhibition efficiency of electrochemical impedance spectroscopy, R_{PO} and R_P are referred to as the polarization resistance of carbon steel without and with the addition of the inhibitor respectively.

$$IE_I\,(\%) = (1 - i_{corr'}/i_{corr}) \times 100 \quad (6)$$

Where, IE = inhibition efficiency of the potentio-dynamic polarization, $i_{corr'}$ and i_{corr} are the corrosion current densities in the absence and presence of the MPLinhibitor respectively. And details of PDP and EIS measurements are presented in tables 4 and 5, and figure 6.

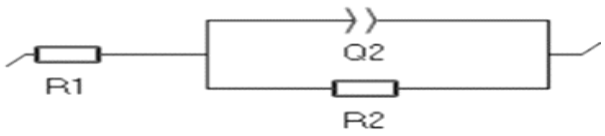

Figure 3. Electrical equivalent circuit used to fit the EIS parameters of the carbon steel in 3.5wt% N aCl without and with the MPL inhibitor

Where, R1=Ohmic drop; R2=charge transfer resistance; Q2=double layer capacitance

2.7.Contact Angle Measurementsof carbon steel in 3.5wt% NaCl

The contact angle measurement seeks to quantify the wetness of the polished carbon steel substrate. The contact angles of the carbon steel specimen in 3.5wt%NaCl solution in the absence and presence of the MPL inhibitor was measured using Optical Tensiometer anddetails of contact angles measured presented in table 6.

2.8. Density Functional Theory, (DFT) Analysis of MPL interfacial adsorption properties on carbon steel

Material studio (version 8.0, BIOVIA) was used to perform density functional theory (DFT) calculations of isolated compounds of the MPL inhibitor molecule using the DMol3 module, quantum chemical parameters such as; E_{LUMO}, E_{HOMO}, energy band gap (ΔE), chemical hardness (η), electronegativity (χ), dipole moment (μ), global Softness (σ), fraction of electron transfer (ΔN) and other important parameters were computed considering Eqs. (7-20), the details of the DFT calculation results are as shown in table 6 while the HOMO and LUMO energies are as shown in figure 7.

E_{HOMO}: Energy of highest occupied molecular orbital

E_{LUMO}: Energy of the lowest unoccupied molecular orbital

Ionization potential,

$$IE = -E_{HOMO} \quad (7)$$

Electron affinity,

$$EA = -E_{LUMO} \quad (8)$$

Energy band gap (eV),

$$\Delta E = E_{LUMO} - E_{HOMO} \quad (9)$$

Electronegativity

$$(eV),\ \chi = (IE+EA)/2 = -(E_{HOMO} + E_{LUMO})/2 \quad (10)$$

Global hardness

$$(eV),\ \eta = -\chi = (E_{LUMO} - E_{HOMO})/2 \quad (11)$$

Global softness $(eV)^{-1}$,

$$\sigma = 1/\eta = -2/(E_{HOMO} - E_{LUMO} \quad (12)$$

Electrophilicity index (eV),

$$\omega = \mu^2/2\eta = \chi^2/2\eta \quad (13)$$

Chemical potential (Debye),

$$\mu \approx -12(I+E) = 12(E_{LUMO}+E_{HOMO}) \quad (14)$$

Nucleophilicity$(eV)^{-1}$,

$$\varepsilon = 1/\omega \quad (15)$$

Electron donating power

$$(eV),\ \omega^- = (3IE+EA)^2 \div 16(IE-EA) \quad (16)$$

Electron accepting power

$$(eV),\ \omega^+ = (IE+3AE)^2 \div 16(IE-EA) \quad (17)$$

Fraction of electron(s) transfer,

$$\Delta N = \chi Fe - \chi Inh.2(\eta Fe + \eta Inh) \quad (18)$$

2.9. Molecular Dynamics (MD) Simulation

The utilization of the forcite module in the Biovia materials studio software (version 8) resource was deployed for this quench molecular dynamics simulation procedure. The simulation was done with Fe(110) crystal with a slab thickness of 3.0Å by importing pure iron framework from the Biovia material studio database while the built tool from the software was used to build the carbon steel surface. It was followed by enlargement of the Fe(110) plane to form a super cell of 35Å x 35Å to create a reasonable space suitable for interaction of the Fe(110) and the MPL extract. A vacuum slab of thickness 48.26Å was built over the Fe (110) plane. The COMPASS (Condensed-phase Optimized Molecular Potential for Atomistic Simulation Studies) force field was adopted in optimizing the structures of all the compounds in the system.

The molecular dynamic simulation was carried out in the constant-temperature, constant-volume

(NVT) ensemble at 298k with a time step of 0.1fs and simulation time of 5.0ps, overall time of loops with the aid of the Anderson thermostat [38, 39]. Where the number of moles (N), volume (V), and temperature (T), are fixed for the system at that time step given and the results of the MD simulation are as shown in figure 9. While the total energy of the system including the binding and interaction energies, the energy of the solution, inhibitor and surface were determined using Eqs.21 and 22.Additionally, the radial distribution function (RDF) was adopted in the evaluation of bond lengths of the interacting molecules while also utilizing the forcite module to perform these calculations. The details of the bond length calculations are shown in table 8.

$$E_{interaction} = E_{total} - (E_{surface} + {}_{solution} + E_{inhibitor}) \quad (21)$$

$$E_{Binding} + E_{interaction} = 0 \quad (22)$$

Where, Eis energy.

3. RESULTS AND DISCUSSION

3.1. FT-IR Analysis of Functional Groups Present in the MPL extract

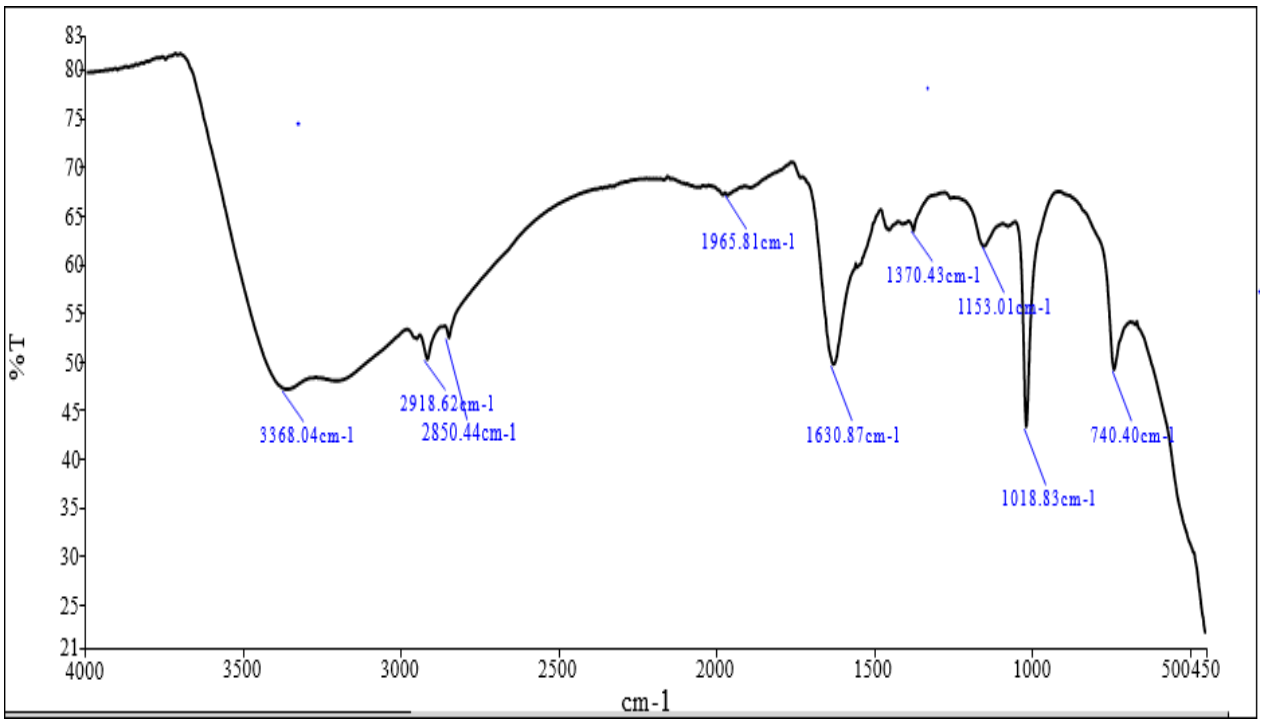

Figure 4. FT-IR vibrations of MPL functional groups showing transmittance, T (%) Vs. wave numbers (cm-1)

Table 2. FT-IR results of functional groups present in MPL extract

S/N	Functional Group	Characteristic Absorption (cm^{-1})
	N-H and O-H	3368.04 (3500-3200)
	C-H	2918.62 (2950-2850)
	C-H	2850.44 (2950-2850)
	C=C	1630.87 (1680-1640)
	Methyl, C-H	1370.43 (1370-1350)
	C-O	1153.01 (1260-1050)
	Aromatic, C-H	740.40 (860-680)

Results of FT-IR analysisof the functional groups present in the MPL extract are as shown in figure 4, the identified absorption bands associated to (N-H) and (O-H) hydrophilic polar functional groups falls between 3500-3200 cm^{-1},while the (C-H) stretching vibrations was noted between 2950-2850cm^{-1}. The vibration of (C=C) stretching was observed at around 1680-1640cm^{-1}, while that corresponding to (methyl C-H) vibration stretching was observed at between 1370-1350 cm^{-1}. The absorption vibrations between 1260-1050cm^{-1} was due to C-O functional group, while the vibrations between 860-680cm-1 was identified as (Aromatic C-H). All the functional groups identified are

electron-donating groups (EDGs) or substituent. EDGs help to increase electron density at the adsorption sites thereby facilitating electron transfer that will enable inhibitor-metal surface interaction. Table 2 shows the functional groups identified in the MPL extract.

3.2. Gravimetric/Weight Loss method

Table 3. (a)Weight loss(g), Corrosion rate (mm/y) of carbon steel and IE (%) of MPL extract(inhibitor) in 3. 5wt% NaCl solution at various Concentrations (g/L) and Exposure time (hrs.)

Conc. (g/L) MPL	1 hr.			6 hr.			24 hr.			48 hr.		
	ΔW(g)	CR (mm/y)	IE(%)	ΔW(g)	CR (mm/y)	IE(%)	ΔW(g)	CR (mm/y)	IE(%)	ΔW(g)	CR (mm/y)	IE(%)
Blank	0.0021± .0003	2.2533		0.0051 ± .0003	0.9121		0.0075± .0003	0.3353		0.0184± .0003	0.4113	
10	0.0018 ± .0005	1.9314	14	0.0045 ± .0003	0.8048	12	0.0046± .0003	0.2057	39	0.0146± .0003	0.3264	21
20	0.0015 ± .0004	1.6095	29	0.0042 ± .0003	0.7511	18	0.0039± .0003	0.1744	48	0.0120± .0003	0.2683	35
40	0.0012 ± .0004	1.2876	43	0.0015 ± .0003	0.2683	71	0.0022± .0003	0.0984	71	0.0117± .0003	0.2615	36
60	0.0010 ± .0006	1.0730	52	0.0014 ± .0003	0.2504	73	0.0017± .0003	0.0760	77	0.0102± .0004	0.2280	45
80	0.0009 ± .0004	0.9657	57	0.0011 ± .0003	0.1967	78	0.0013± .0003	0.0581	83	0.0099± .0003	0.2213	46
100	0.0007 ± .0003	0.7511	67	0.0010 ± .0002	0.1788	80	0.0008± .0002	0.0358	89	0.0071± .0004	0.1587	61

Table 3(b). Continuation of table 4a

Conc. (g/L) MPL	72 hr.			96 hr.			120 hr.		
	ΔW(g)	CR (mm/y)	IE (%)	ΔW(g)	CR (mm/y)	IE (%)	ΔW(g)	CR (mm/y)	IE (%)
Blank	0.0234 ±.0003	0.3487		0.0491 ±.0003	0.5488		0.0986 ±.0003	0.8817	
10	0.0185 ±.0003	0.2757	21	0.0307 ±.0003	0.3431	37	0.0424 ±.0004	0.3791	57
20	0.0165 ±.0003	0.2459	29	0.0300 ±.0003	0.3353	39	0.0280 ±.0003	0.2504	72
40	0.0150 ±.0004	0.2235	36	0.0204 ±.0003	0.2280	58	0.0216 ±.0003	0.1931	78
60	0.0138 ±.0003	0.2057	41	0.0191 ±.0003	0.2135	61	0.0200 ±.0003	0.1788	80
80	0.0103 ±.0003	0.1535	56	0.0134 ±.0004	0.1498	73	0.0152 ±.0004	0.1359	85
100	0.0092 ±.0004	0.1371	61	0.0129 ±.0004	0.1442	74	0.0091 ±.0003	0.0823	91

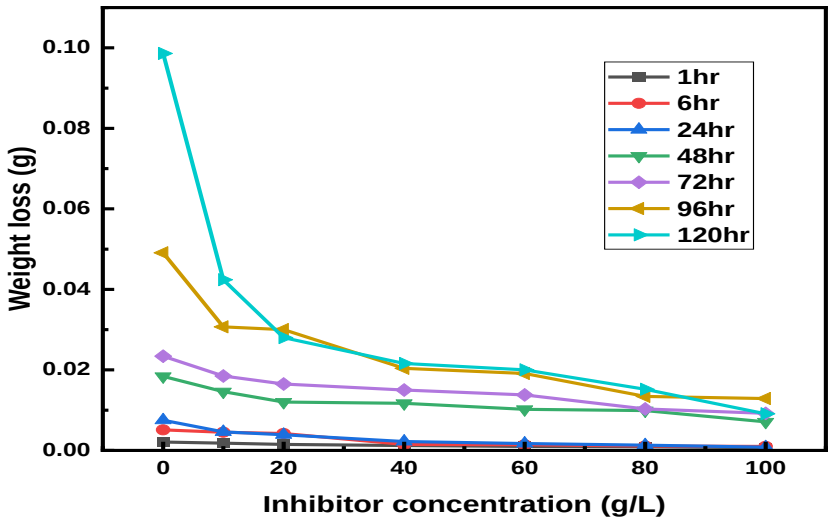
Weight loss (g)
Inhibitor concentration (g/L)
1hr
6hr
24hr
48hr
72hr
96hr
120hr

(a)

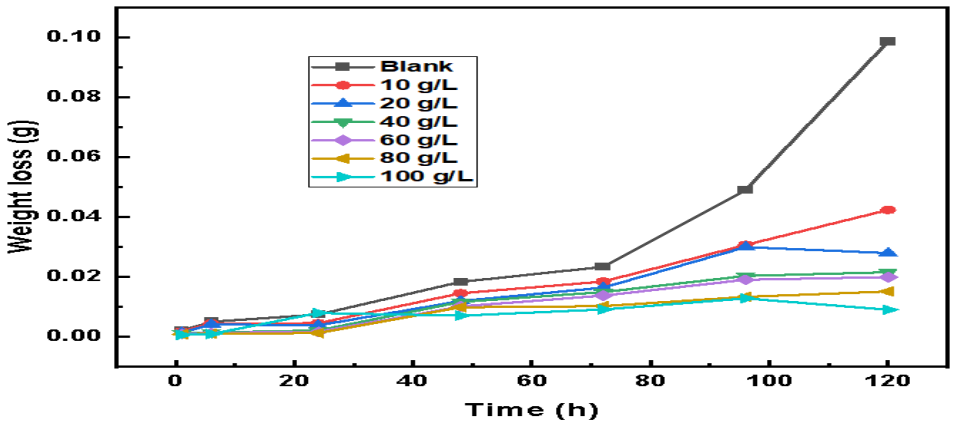
Weight loss (g)
Time (h)
Blank
10 g/L
20 g/L
40 g/L
60 g/L
80 g/L
100 g/L

(b)

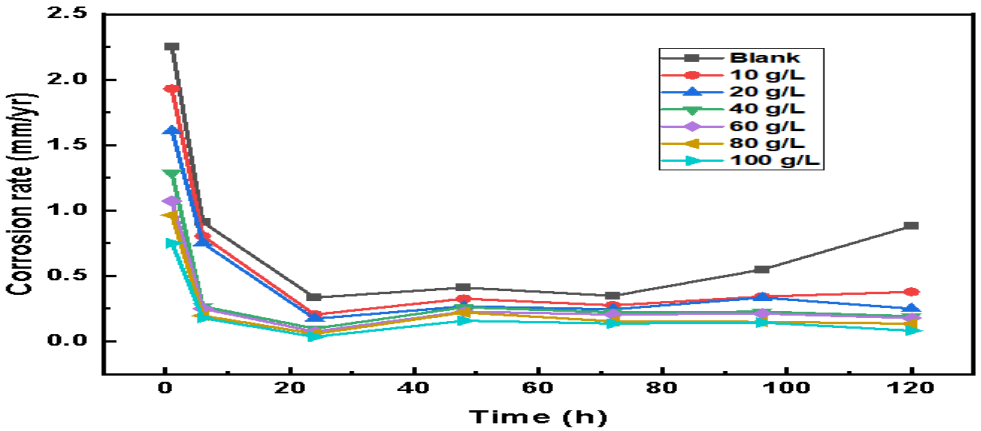
Corrosion rate (mm/yr)
Time (h)
Blank
10 g/L
20 g/L
40 g/L
60 g/L
80 g/L
100 g/L

(c)

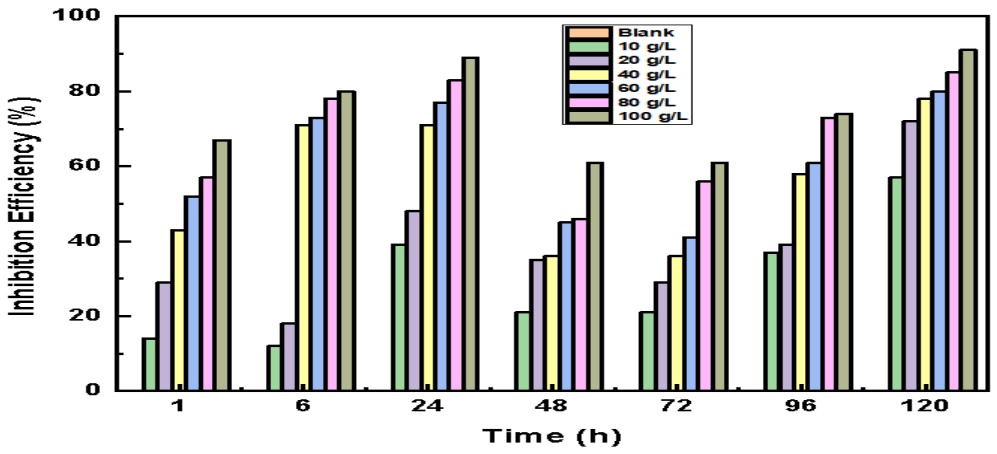

(d)

Figure 5. Effect of MPL concentration on carbon steel immersed in 3.5 wt% NaCl solutions in the absence and presence of different concentrations of MPL inhibitor at 25°C: (a) Weight loss Vs Inhibitor Conc., (b) Weight loss Vs Time, (c) Corrosion rate Vs Time (d) Inhibition Efficiency Vs Time for 120hrs immersion of carbon steel in 3.5wt.% NaCl

The effect of the MPL inhibitor on Carbon Steel in 3.5wt.% NaCl solution is shown in figure 5. The parameters such as weight loss, corrosion rate and inhibition efficiency in the absence and presence of the various concentrations of the MPL inhibitor in 3.5wt% NaCl solution over the immersion time 1hr, 6hrs, 24hrs, 48hrs, 72hrs, 96hrs and 120hrs can also be seen on tables 3 (a) and (b). Figure 5a shows weight loss against MPL inhibitor concentration, it is observed that as the MPL inhibitor concentration increases, the weight loss decreases. Looking at figure 5b, it is observed that as time goes on the weight loss decreased as the MPL inhibitor concentration was increased. Likewise, observing figure 5c,it can be observed that as the MPL inhibitor concentration increased, the corrosion rate decreases with time. From figure 5d, looking at the inhibition efficiency it is seen that it increased as inhibitor concentration increased with time and that at 100g/L concentration of MPL, the inhibition efficiency was observed to be 91% at an immersion time of 120 hours. As expected, this led to a decrease in corrosion rate from 0.8817 mm/y to 0.0823 mm/y. Likewise, the weight loss experienced by the test specimen decreased from 0.0986g to 0.0091g.

3.3. Electrochemical Investigation

In this section the results of electrochemical investigation which involves the potentiodynamic polarization and electrochemical impedance spectroscopy (EIS) analyses are presented. The equivalent circuit model for the EIS is shown in figure 3

Table 4. Polarization parameters of carbon steel with various MPL extract concentrations in seawater environment at 298K

	Ecorr (mV)	Icorr (μA)	β c (mV)	β a (mV)	corrosion rate (mm/y)	IE (%)
Blank	-694.347	87.403	2026	208.5	0.440 4	
10g/L	- 686.940	22.108	9 701	155.2	0.260 3	74.71
20g/L	-471.103	21.679	9624	52.8	0.255 3	75.20
40g/L	-626.121	20.991	50 72	110.0	0.247 2	75.98
60g/L	-481.808	19.979	2190	63.7	0.237 3	77.14
80g/L	-700.390	16.342	15 05	82.9	0.192 4	81.30
100g/L	-705.223	8.615	1752	77.1	0.136 8	90.14

Table 5. Electrochemical impedance spectroscopy parameters of carbon steel with various MPL extract concentrations in seawater environment at 298K

	R1 (Ohm)	Q2 (F.s^(a - 1))	a2	R2 (Ohm)	IE%
Control	8.9458	0.00064	0.7870	1140	
10 g/L	8.8653	0.00078	0.8041	5403	79.0

20 g/L	7.5921	0.00034	0.7792	5516	79.3
40 g/L	9.3170	0.00032	0.7805	5586	79.6
60 g/L	6.1062	0.00043	0.7764	5593	79.6
80 g/L	8.0875	0.00070	0.7759	6694	83.0
100 g/L	7.6941	0.00080	0.7914	7112	84.0

The corrosion parameters obtained from potentiodynamic polarization (PDP) are presented in table 4 while figure 6a shows the Tafel plots which is related to the activation energy of the reaction, thereby indicating the reaction rate. Considering table 4, the concentration of MPL extract at 100g/L showed the corrosion rate of about 0.1mm/y with an efficiency of 90.1%. This result is in line with the shifting of the polarization curves towards more negative values which indicate that as the MPL concentration increased from 10g/L to 100g/L there was a reduction in corrosion current density. The cathodic branch of the Tafel plot as in figure 6a clearly shows the transition from activation-controlled reaction which limiting step is the transfer of electrons (oxidation) to the surface of the metal, to diffusion-controlled reaction which limiting step is the transport of chemical species such as diffusion (reduction) of oxygen to water. Again, looking at the polarization slopes of all the MPL concentrations of the Tafel plots, it is observed that the slopes shift towards negative current densities with the 100g/L shifting to the most negative value indicating reduction in corrosion rate. The ability of MPL inhibitor to control the activation reaction (oxidation) and the diffusion reaction (oxygen reduction) makes it a mixed-type corrosion inhibitor. A close observation showed hydrogen evolution due to limited oxygen to get to the surface of the metal thereby limiting current density and hence corrosion rate.

The electrochemical impedance spectroscopy (EIS) of carbon steel in 3.5wt% NaCl solution in the absence and presence of MPL extract-based inhibitor at various concentrations was also investigated and the parameters are presented in table 5. The Nyquist plot, Bode plot and Phase angle are shown in figures 6b, 6c and 6d respectively. The Nyquist plot is explained using an equivalent circuit model as shown in figure 3. The semicircular shape of the Nyquist plot demonstrates the charge transfer resistance at the metal/electrolyte interface, with the semicircle diameter of each concentration corresponding to the extent of corrosion resistance. As the concentration of the MPL increase from 10g/L to 100g/L, the diameters of the semicircles also increased, indicating better corrosion resistance. The largest semicircle is observed at 100g/L of MPL concentration showing the highest corrosion resistance which is in line with the inhibition efficiency of 84% as shown in table 5. Also, the polarization resistance, Rp is highest at 100g/L of MPL concentration indicating slower corrosion rate and absence of pure capacitance response. From figure 6b, it is observed that as the MPL concentration increased, the Nyquist plot showed a widened diameter and increased peak heights indicating a higher charge transfer resistance (R_{ct}) and large surface coverage. A one-time constant was detected in Bode diagrams and phase angle, see figure 6(c, d) with a characteristic increase in absolute impedance values and decrease in phase angle confirming the prevalence of charge transfer mechanism over the electrolyte/substrate interface.

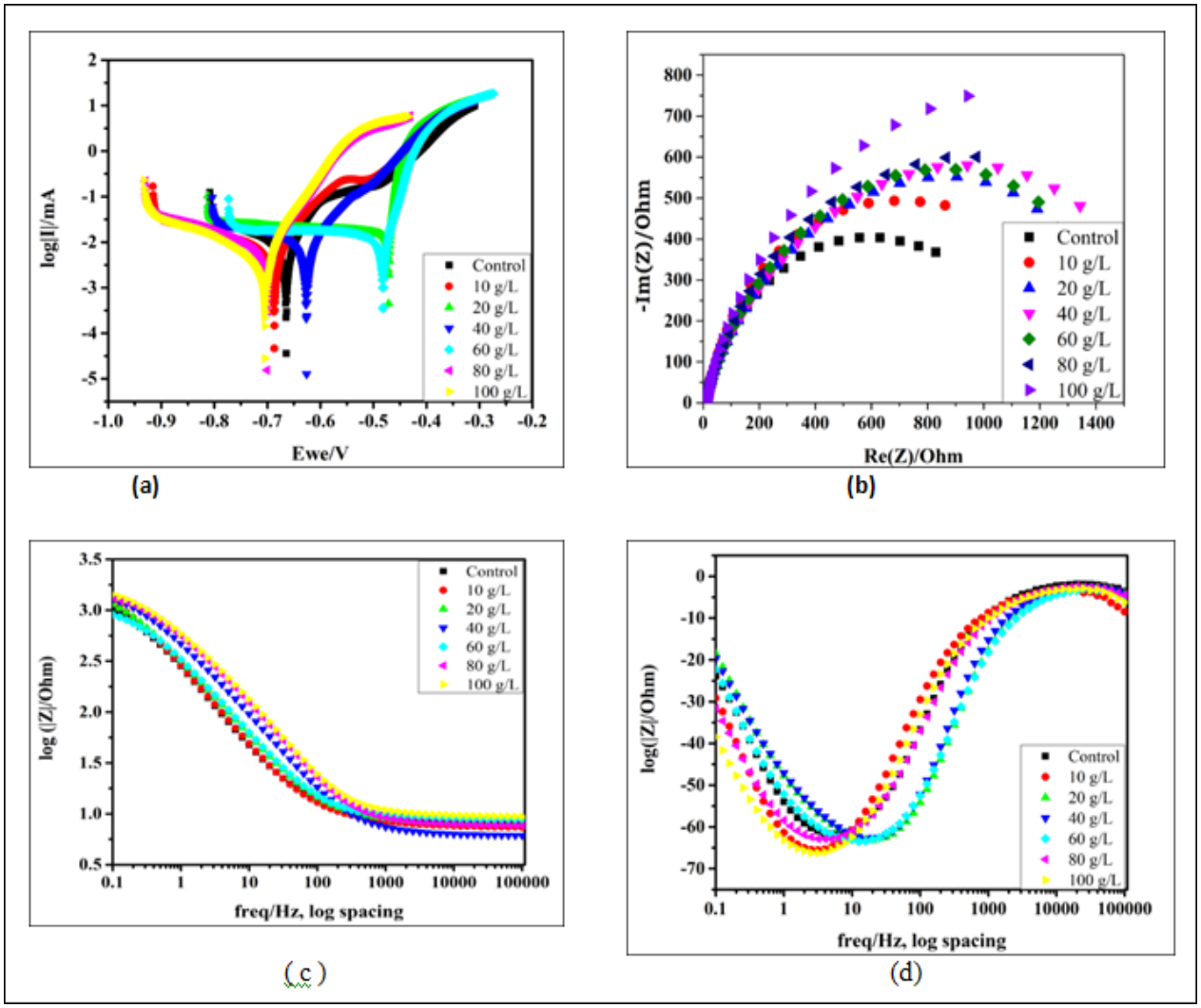

Figure 6. (a) Tafel, (b)Nyquist,(c) Bode and (d) Phase angle, plots of carbon steel in 3.5wt% NaCl with and without various concentrations of MPL at Ecorr after 45 mins immersion

3.4. Contact angle measurements

The contact angle measurement seeks to quantify the wetness of the polished carbon steel substrate, the carbon steel in 3.5wt%NaCl solution in the presence and absence of the MPL inhibitor. The contact angle measurements and properties are presented in table 6.

Table 6: Contact angle measurements/properties of dry polished carbon steel, and carbon steel immersed in 3.5wt%NaCl without MPL and carbon steel immersed in 3.5wt%NaCl with MPL inhibitor

Property	Dry polished Carbon Steel	Carbon steel immersed in 3.5wt% NaCl	Carbon steel immersed in 3.5wt%NaCl + 100g/L MPL
			
Contact angle value (°)	68.19	76.20	152.42
Nature of wettness	Hydrophilic	Hydrophilic	Superhydrophobic
Wettability	Good	Good	Poor
Solid surface free energy	High	High	Low

From table 6 it is observed that the dry polished carbon steel surface has a high free energy, a low contact angle of 68.19° indicating that the surface is favorable to wetting, hence hydrophilic, therefore, exposing the surface to corrosive ions from moisture. Likewise, it is observed that the surface of carbon steel immersed in 3.5wt%NaCl in the absence of the MPL inhibitor also has a high free energy, a low contact angle of 76.20° also indicating that the surface is favorable to wetting showing good wetting properties, hence hydrophilic as well, therefore prone to corrosive chloride ions in the solution. However, looking at the same table, it is observed that the surface of carbon steel immersed in 3.5wt%NaCl in the presence of 100g/L MPL has a low free energy and high contact angle of 152.42° indicating that the surface is not favorable to wetting showing poor wetting properties, hence superhydrophobic. This can be attributed to the thin film (Langmuir films) from the MPL inhibitor which adsorbed on the surface of the metal effectively shielding the surface from corrosive chloride ions and enhancing its water repellant properties.

3.5. Theoretical (DFT) Analysis of MPL Inhibitory Properties

The quantum chemical properties were obtained after geometric optimization with respect to the DMol3 model at the DFT level. The optimized molecular structures of the studied MPL isolated molecules are as shown in figure 7. The computed values of the quantum chemical parameters for the isolated molecules present in the MPL extract are stated in table 7. Generally, the global reactivity of molecules can be estimated from the energies of the frontier molecular orbital [40-42] such as: HOMO orbital which represents the ability of a molecule to lose electrons, and LUMO orbital which indicates the ability of a molecule to accept electrons. Considering table 7, all the quantum chemical descriptors in this section can be explained.

Table 7. Quantum Chemical Descriptors for the isolated compounds in MPL molecule

Descriptor	M1	M2	M3	M4	M5	M6
EHOMO	-6.505	-4.939	-5.973	-6.727	-5.952	-5.73
ELUMO	-1.871	-0.879	0.38	0.362	0.958	-0.601
ΔE	4.634	4.06	6.353	7.089	6.91	5.129
X	4.188	2.909	2.7965	3.1825	2.497	3.1655
μ	-4.188	-2.909	-2.7965	-3.1825	-2.497	-3.1655
H	2.317	2.03	3.1765	3.5445	3.455	2.5645
Σ	0.431593	0.492611	0.314812	0.282127	0.289436	0.38994
Ω	3.784925	2.084306	1.230979	1.428736	0.902317	1.953673
ϵ	0.264206	0.479776	0.812361	0.69992	1.108258	0.511856
ω+	1.98055	0.883556	0.229792	0.280548	0.085692	0.691486
ω-	6.16855	3.792556	3.026292	3.463048	2.582692	3.856986
ΔN	0.903755	0.716502	0.440186	0.448935	0.36136	0.617177

Legend: M = Isolated compounds of the MPL molecule

Isolated molecule	Optimized structure	HOMO Orbital	LUMO Orbital

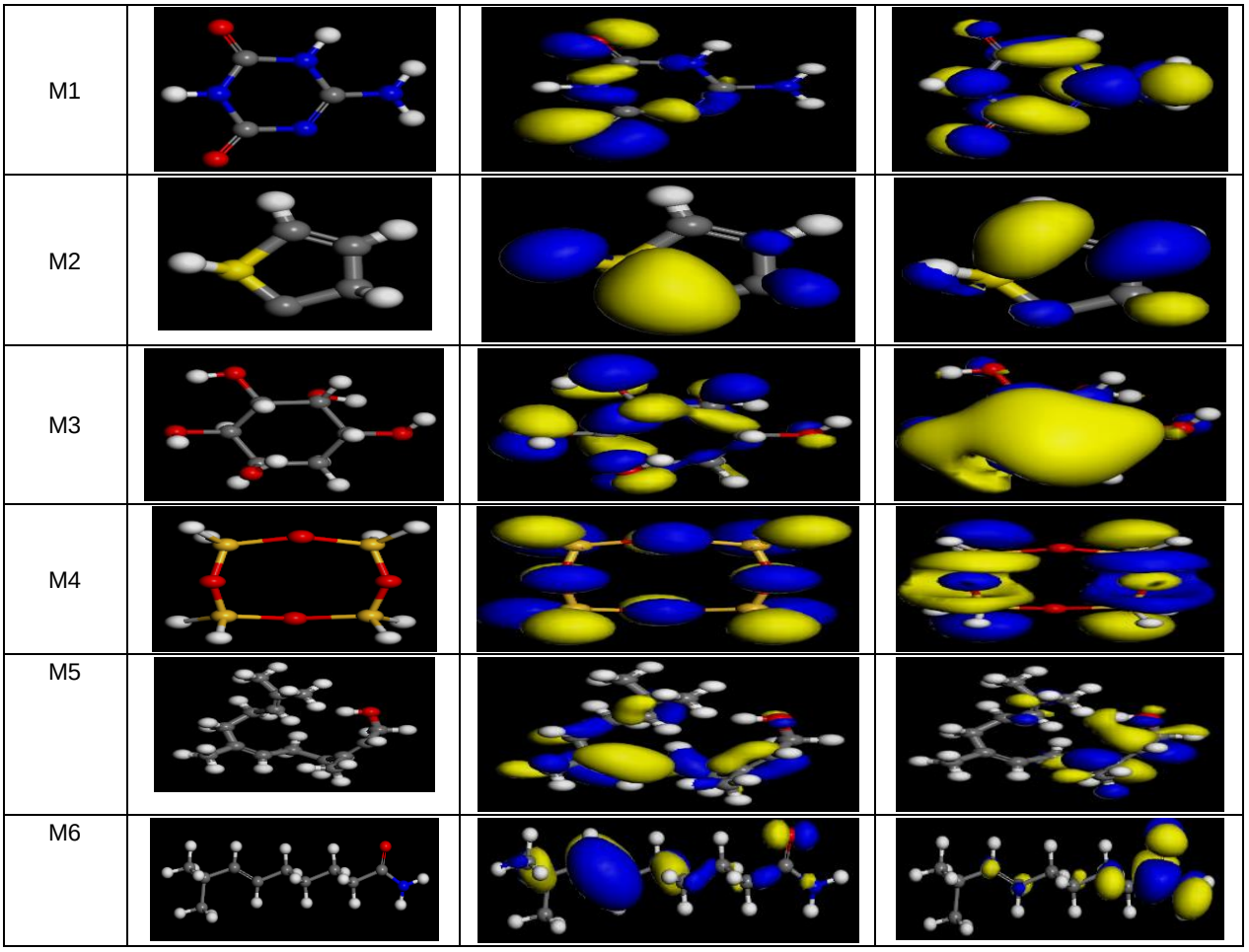

Legend: Oxygen (O), ● =red, Carbon (C) ● =gray, Sulphur (S) ●= yellow, Nitrogen (N) ● =blue, Hydrogen (H),●= white ; M = Isolated compounds of the MPL molecule

Figure 7. Shows optimized structures, HOMO and LUMO densities of isolated compounds in MPL inhibitor molecule

The quantum chemical properties were obtained after geometric optimization with respect to the DMol3 model at the DFT level. The optimized molecular structures of the studied MPL isolated molecules are as shown in figure 7. The computed values of the quantum chemical parameters for the isolated molecules present in the MPL extract are stated in table 7. Generally, the global reactivity of molecules can be estimated from the energies of the frontier molecular orbital [40-42] such as: HOMO orbital which represents the ability of a molecule to lose electrons, and LUMO orbital which indicates the ability of a molecule to accept electrons. Considering table 7, all the quantum chemical descriptors in this section can be explained.

The results from table 7 shows that the E_{HOMO} values did increase in the following order: M4 < M1< M3 < M5 < M6 < M2. Therefore, the ability to contribute to electron donation to the vacant d-orbital of the carbon steel surface is expected to follow the same order.

On the other hand, also referring to table 7, the E_{LUMO} values did decrease in the following order: M5 < M3 < M4 < M6 < M2 < M1, and thus the ability to accept electrons would be expected to follow the same order.

The energy band gap, ΔE represents the difference between the energy of HOMO and LUMO orbital. The ΔE values of the studied compounds decreased in the following order: M4 > M5 > M3 > M6 > M1 > M2. The electronegativity (χ) values for the isolated molecules decreased in the following order: M5 < M3 < M2 < M6 < M4 < M1 and their individual contribution favoring effective inhibition efficiency for the MPL inhibitor in that same order.

In the same vein, the chemical hardness (η), decreased in the following order: M2 < M1 < M6 <

M3 < M5 < M4 making the metal act like a Lewis acid and hence as an electron acceptor.

While the values of global softness (σ) increased in the following order: M2 > M1> M6 > M3 > M5 > M4. As a result, making the MPL inhibitor act as a Lewis base and hence an electron donor to the d-orbital of the metal which acts as a Lewis acid, hence electron acceptor. The dipole moment increased as follows: M5 > M3 > M2 > M6 > M4 > M1 showing the tendency of the MPL inhibitor to adsorb on the carbon steel metal surface.

Considering the electrophilic (ω) and nucleophilic (ϵ) descriptors, as presented in table 7, it is observed that the values of (ω) decreased in the following order; M5< M3 < M4 < M6 < M2 < M1 while the values (ϵ) increased in the following order; M5 > M3 > M4 > M6 > M2 > M1 respectively, therefore making all the MPL isolated inhibitor molecules contribute positively to electron transfer to the carbon steel d-orbitalLikewise, considering the electron donating (ω^-) and the electron accepting (ω^+) power descriptors, from table 7, it can be observed that all the values of (ω+) for the isolated molecules of the MPL are less than the values of (ω-) showing their better proclivity to give electrons than accepting.

Subsequently, the ΔN descriptor which is the fraction of electrons transferred, gives us an indication of the capacity to donate electrons to the metal surface. According to Lukovits et al, if ΔN<3.6 then the inhibition efficiency of the inhibitor molecules is increasing with electron affinity on the metal surface [43]. Hence improved electron releasing power was replaced by electron-donating group by altering a hydrogen atom of the aromatic ring. Consequently, in this study, all the isolated MPL inhibitor molecules studied have ΔN values less than 3.6 which indicate that the inhibitor's molecules are electron donors and the metal surface is an acceptor.

The HOMO and LUMO densities of the isolated compounds are presented in figure 7. It can be seen from the figure that the MPL has shown the presence of electron-rich centers, heteroatoms and polar groups which are responsible for both chemical and physical adsorption, suggestive of a mixed-type inhibitor. According to Miralrio and Espinoza-Vazquez, electron-rich regions and heteroatoms have been found to be responsible for chemisorption. Meanwhile, physisorption is associated with the presence of polar functional groups in a molecule [44].

3.6. MD simulation of isolated compounds in MPL inhibitor molecule onto carbon steel in 3.5wt% NaCl solution

From figure 8, it is observed that the orientation of the MPL inhibitor molecules on the metal surface is planar as such it covers a larger part of the metallic surface contributing to large surface coverage and acts as a superior corrosion inhibitor [1,2]. In this case, the presence of heteroatoms and electron donating substituent groups forced the MPL inhibitor to attain a planar orientation on the carbon steel surface as such indicating effectiveness in corrosion inhibition with a high adsorption energy value -268.172 Kcal/mol indicating that the studied molecules adsorb easily onto the metal surface and exhibit strong intermolecular interactions.

Compound	Side view	Top view	Adsorption energy
M1	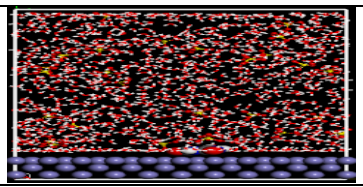	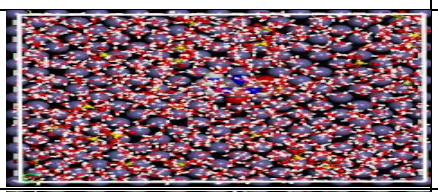	-60.549
M2	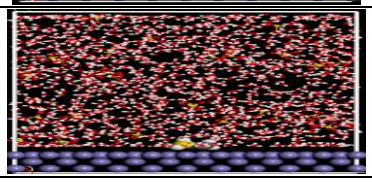	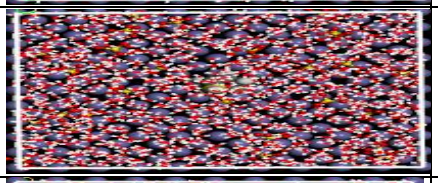	-34.641
M3	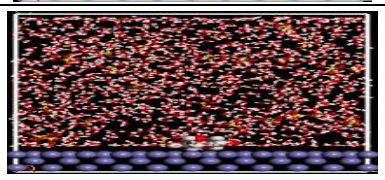	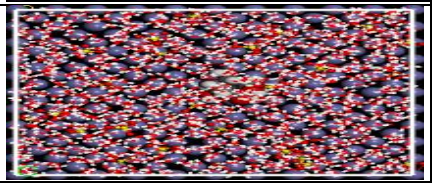	-54.144

M4	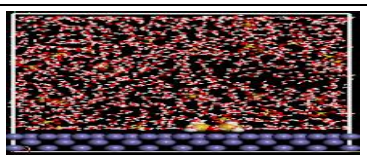	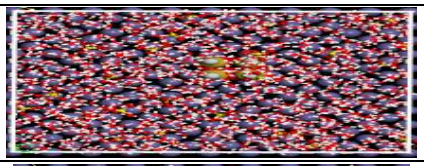	-61.804
M5	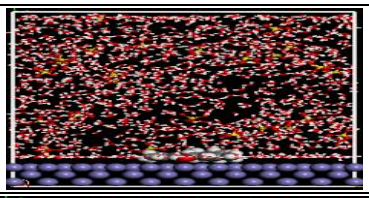	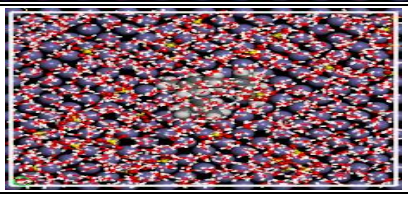	-116.344
M6		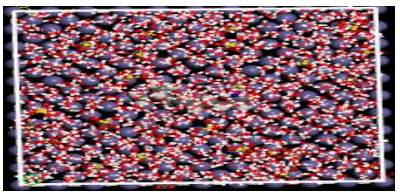	-88.495
Extract super structure (all the components)	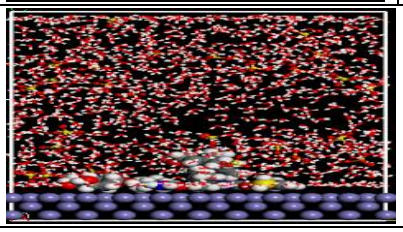	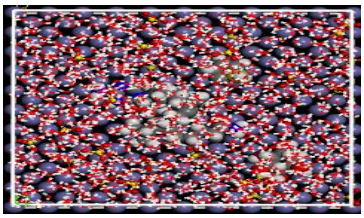	-268.172

Legend:  = Metal surface;  = MPL molecule; Na^+ = ● Cl^- = ●

Figure 8. Equilibrium adsorption mode of isolated compounds of the MPL molecule onto Fe (110) surface showing top and side views

3.6.1. Radial Distribution Function (RDF) for MPL in 3.5wt% NaCl solution on carbon steel

Table 8. Bond length analysis of MPL inhibitor molecule in 3.5wt% NaCl medium via RDF

Interaction	Bond length (A)
Fe (110)-N	2.970
Fe (110)-O	3.49
Fe (110)-S	3.27
Fe (110)-Si	3.19
Fe (110)-C	2.97

Legend: Fe (110) = Iron; N = Nitrogen; O = Oxygen; S = Sulfur; Si = Silicon; C = Carbon

The radial distribution function (RDF) which helps to determine the bond lengths of MPL interacting molecules can be calculated using MD simulation. The interaction between two or more molecules can be a chemical adsorption (chemisorption) or a physical adsorption (physisorption). Chemical adsorption is associated with shorter bond length between 1.0 and 3.5 Å and gives high bond strength, while physical adsorption is marked by bond length longer than 3.5 Å and correspondingly indicates lower bond strength [45-49]. In this case, the values of the bond lengths determined by the RDF analysis are stated in Table 8 and can be seen that all the atoms of the MPL molecule were chemically adsorbed on the steel surface indicating a strong interfacial interaction between the substrate and the inhibitor.

4. CONCLUSION

In conclusion, MPL extract-based inhibitor has demonstrated effective corrosion inhibition protection of carbon steel in 3.5wt%NaCl solution, functioning as a mixed-type corrosion inhibitor due to the presence of electron-rich centers, heteroatoms, polar functional groups andshowing inhibition efficiency of between 84% and 91% at 100g/L concentration in 120h with a large surface coverage of 0.91. Apart from being a good corrosion inhibitor, MPL has also shown very unique properties typical of a surfactant with Langmuir films that contains both hydrophilic and hydrophobic properties attributed to the presence of saponins in its molecule. AsSURFACTANT it is very important in the oil and gas industry, contributing significantly to oil and gas operations as follows:

- It is used as drilling mud additives during the process of drilling and well completions.

- Also used in the process of enhanced oil recovery as surface active agents to reduce interfacial tension between oil and water, alter rock wettability and improve the displacement efficiency of oil.
- Again, it is used as emulsifier, demulsifier and solubilizing agents during oil production, processing and oil spillage cleaning processes respectively.
- Furthermore, MPL is inexpensive, environment-friendly and its use aligns with the growing emphasis on sustainability in industrial practices, offering a promising opportunity for corrosion management without compromising environmental and health standards, hence, contributing greatly to knowledge.Future studies should seek to find out if MPL can be used to inhibit scale in oil and gas drilling operations.

Author Contributions

All authors contributed to the conceptualization and design of the study. Computational simulation studies were carried out by Osuani F. Idema; Innocent O. Arukalam and Chigoziri N. Njoku. First draft was done by Osuani F. Idema and revising/correction were done by Anyiam N. Chioma; Ikenna B. Onyeachu and Ifeyinwa C. Ekeke. Supervision, Data analysis and interpretation were done by Malik Abdulwahaband Emeka E. Oguzie. All authors reviewed and approved the final manuscript.

Acknowledgements

The authors are grateful for the research support from the Africa Centre of Excellence in Future Energies and Electrochemical Systems (ACE-FUELS), Federal University of Technology Owerri (FUTO), Nigeria for the provision of the software and other materials including their general research laboratory used for the study.

Conflict of Interest

The authors declare that there are no competing interests whatsoever, be it commercial, financial or otherwise regarding the publication of this original article.

5. REFERENCES

[1] C. Verma, E. E. Ebenso, M. A. Quraishi,C. M. Hussain(2021) Recent developments in sustainable corrosion inhibitors: design, performance and industrial scale applications. Mater. Adv., 2,3806–3850

[2] G. Jacobson (2016) NACE International, Houston, Texas, USA ©**2016** by NACE International, 15835 Park Ten Place, Houston, TX 77084

[3] F. El-Hajjaji, M. Messali, A. Aljuhani, M. R. Aouad, B. Hammouti, M. E. Belghiti,D. S. Chauhan (2018) Pyridazinium-based ionic liquids as novel and green corrosion inhibitors of carbon steel in acid medium: Electrochemical and molecular dynamics simulation studies. J. Mol. Liq.,249, 997-1008

[4] N. Hossain, M. C. Asaduzzaman,M. Kchaou (2021) Anoverview of green corrosion inhibitors for sustainable and environment friendly industrial development.J. Adhes. Sci. Technol.,35(7), 673–690

[5] A. K. Satapathy, G. Gunasekaran, S. C Sahoo, K. Amit,P. V. Rodrigues(2009) Corrosion inhibition by Justicia gendarussa plant extract in hydrochloric acid solution.Corros.Sci.,51(12), 2848–2856. doi: 10.1016/j.corsci.2009.08.016

[6] N. Chaubey, A. Qurashi, D. S. Chauhan, M. A. Quraishi(2021) Frontiers and advances in green and sustainable inhibitors for corrosion applications: A critical review.J. Mol. Liq.,321, 114385. doi: 10.1016/j.molliq.2020.114385

[7] A. Toghan, H. S. Gadow, A. Fawzy, H. Alhussain,H. Salah(2023) Adsorption Mechanism, Kinetics, Thermodynamics, and Anticorrosion Performance of a New Thiophene Derivative for C-Steel in a 1.0 M HCl: Experimental and Computational Approaches. Metals 13(9),1565.doi: 10.3390/met13091565.

[8] H. L. Y. Sin, A. A. Rahim,C. Y Gan, B. Saad, M. I. Salleh,M. Umeda(2017) Aquilaria subintergra leaves extracts as sustainable mild steel corrosion inhibitors in HCl,*Meas*. J. Int.Meas. Confed.,109, 334–345.doi: 10.1016/j.measurement.2017.05.045.

[9] N. Patni, S. Agarwal, P. Shah(2013)Greener Approach towards Corrosion Inhibition. Chinese J. Eng., 2013, 1–10.

[10] P. B. Raja and M. G. Sethuraman(2008) Natural products as corrosion inhibitor for metals in corrosive media — A review. Mat. Letters.,62(1), 113.doi: 10.1016/j.matlet.2007.04.079.

[11] S. H. Alrefaee, K. Y. Rhee, C. Verma, M. A. Quraishi and E. E. Ebenso(2021) Challenges and advantages of using plant extract as inhibitors in modern corrosion inhibition systems: Recent advancements.J. Mol. Liq., 321, 114666. doi: 10.1016/j.molliq.2020.114666.

[12] Q. Wang, B. Tan, H. Bao, Y. Xie, Y. Mou, P. Li, D. Chen, Y. Shi, X. Li and W. Yang (2019) Evaluation of Ficus tikoua leaves extract as an eco-friendly corrosion inhibitor for carbon steel in HCl media.Bio electrochemistry,128, 49-55. doi: 10.1016/j.bioelechem.2019.03.001.

[13]S. Chen, S. Chen, B. Zhu, C. Huang, W(2020) Magnolia grandiflora leaves extract as a novel environmentally friendly inhibitor for Q235 steel corrosion in 1 M HCl: Combining experimental and theoretical researches.J. Mol. Liq.,*311*, 113312. doi: 10.1016/j.molliq.2020.113312.

[14]A. Carmona-Hernandez, M. C. Barreda-Serrano, H. A. Saldarriaga-Noreña, R. López-Sesenes, J. G. González-Rodríguez, E. Mejía-Sánchez, J. A. Ramírez-Cano, R. Orozco-Cruz and R. Galván-Martínez (2024) Insight into the Corrosion Inhibition Performance of Pistia stratiotes Leaf Extract as a Novel Eco-Friendly Corrosion Inhibitor for Mild Steel in 1 M HCl Solution.Molecules, 5243. doi: 10.3390/molecules29225243.

[15] M. Sabiha, Y. Kerroum, M. El Hawary, M. Boudalia, A. Bellaouchou, O. Hammani and H. M. A. Amin(2025) Investigating the Adsorption and Corrosion Protection Efficacy and Mechanism of Marjoram Extract on Mild Steel in HCl

Medium.Molecules 30(2), 272. doi:10.3390/molecules30020272.

[16]A. Elyoussfi, H. E. Hassouni, F. Benhiba, H. Outada, H. Amhamdi, A. Zarrouk, A. Romane and A. Dafali(2024) Origanum Grosii Extracts as Novel Eco-Friendly Corrosion Inhibitors for Mild Steel In HCl Medium.Chem Biodivers., 21(5), e202301915.

[17]S. Haddou, K. Zaidi, O. Dagdag, A. Hbika, M. Adil Mahraz, M. Bouhrim, A. S. Alqahtani , O. M. Noman, H. Kim, A. Aouniti, B. Hammouti, A. Chahine (2025) Theoretical and Electrochemical Evaluation of Cannabis Sativa L. Extracts as Corrosion Inhibitors for Mild Steel in Acidic Medium.Chemistry Open, 14(5), e202400273.

[18]M. Tabyaoui, M. Tourabi, H. Zarrok, C. Jama, F. Benhiba, A. Zarrouk, F. Bentiss (2024) Citrullus colocynthisfruit extract as effective eco-friendly corrosion inhibitor in a hydrochloric acid pickling medium for carbon steel by using both experimental and theoretical studies. Environmental Science and Pollution Research, 31 (31) 43757–43780, doi: 10.1007/s11356-024-34055-6

[19]I. Nadi, Z. Belattmania, B. Sabour, A. Reani, A. Sahibed-Dine, C. Jama, F. Bentiss (2019) Sargassum muticum extract based on alginate biopolymer as a new efficient biological corrosion inhibitor for carbon steel in hydrochloric acid pickling environment: Gravimetric, electrochemical and surface studies. International Journal of Biological Macromolecules, (141) 137–149, Dec. 2019, doi: 10.1016/j.ijbiomac.2019.08.253

[20] M. Dent, R. Fuchs-Godec (2021)Sage Extract as a Natural Source of Corrosion Inhibitor for Tinplate in 3.0 % NaCl. Food Technology and Biotechnology, 59(4),413–421, Sep. 2021, doi: 10.17113/ftb.59.04.21.7026.

[21]A. Cojocaru, G. E. Badea, I. Maior, S. Dzitac, O. D. Stănășel, M. Sebeșan, C. D. Ionaș, P. Creț (2025) Electrochemical Investigations of Galium verum Ethanolic Extract as a Steel Corrosion Eco-Inhibitor in the Acid Media: An Unexpected Versatility of Plant Chemistry. Materials, 18(9) 2078, doi: 10.3390/ma18092078

[22]M. Adil Mahraz, R. Salim, E. H. Loukili, A. Assouguem, M. Kara, R. Ullah, A. Bari, H. Fidan, A. Laftouhi, A. Mounadi Idrissi, B. Hammouti, Z. Rais, M. Taleb (2024) Exploratory evaluation supported by experimental and modeling approaches of Inula viscosa root extract as a potent corrosion inhibitor for mild steel in a 1 M HCl solution.Open Life Sciences, 19(1), Jan. 2024, doi: 10.1515/biol-2022-0879

[23] C. Akalezi, A. Maduabuchi, C. Enenebaku, E. E. Oguzie (2020) Experimental and DFT evaluation of adsorption and inhibitive properties of Moringa oliefera extract on mild steel corrosion in acidic media. Arabian Journal of Chemistry, 13 (12) 9270–9282, Dec. 2020, doi: 10.1016/j.arabjc.2020.11.010.

[24]. M. A. Mahraz, R. Salim, E. H. Loukili, A. Laftouhi, S. Haddou, A. Elrherabi, M. Bouhrim, R. N. Herqash, A. A. Shahat, B. Eto, B. Hammouti, Z. Rais, M. Taleb (2025) Ephedra fragilis plant extract: A groundbreaking corrosion inhibitor for mild steel in acidic environments – electrochemical, EDX, DFT, and Monte Carlo studies. Open Life Sciences, 20(1), Jan. 2025, doi: 10.1515/biol-2022-1050

[25]E. G. Asuquo, C. E. Udobi,*Ed Tsai-Ching Hsu (2016)* Antibacterial and toxicity studies of the ethanol extract of Musa paradisiaca leaf. Cogent Biology, 2(1), 1219248, Aug. 2016, doi: 10.1080/23312025.2016.1219248

[26]V. Galani (2019)Investigation of Antistress Activity of Operculina Terpethum Roots using Various Experimental Models. International Journal of Pharmacognosy & Chinese Medicine, vol. 3, no. 3, pp. 1–9, 2019, doi: 10.23880/ipcm-16000180

[27]A. Mahmood, N. Ngah, M. N. Omar (2011) Effects of bioactive constituents extracted from Musa x paradisiaca flower on milk production in Vivo. International Journal of Evidence-Based Healthcare, vol. 9,(3), 313, Sep. 2011, doi: 10.1097/01258363-201109000-00064

[28]P. C. Onyenekwe, O. E. Okereke, S. O. Owolewa (2013) Phytochemical Screening and Effect of & ltem & gt;Musa paradisiacal & lt;/em> Stem Extrude on Rat Haematological Parameters. Current Research Journal of Biological Sciences, 5(1) 26–29, Jan. 2013, doi: 10.19026/crjbs.5.5468.

[29]A. Mishra, K. R. C. Reddy, S. K. Maurya, A. Seth,D. N. S. Gautam (2017) Int. J. Green Pharm, 11, 74

[30] H. O. Edeoga, D. E. Okwu, B. O. Mbaebie (2005) Phytochemical constituents of some Nigerian medicinal plants. African Journal of Biotechnology, vol. 4(7) 685–688, May 2005, doi: 10.5897/ajb2005.000-3127

[31]A.T. Adeolu,D. O. Enesi (2013) International Research Journal of Plant Science. International Research Journal of Plant Science, 4(9), doi: 10.14303/irjps.2013.054

[32] I.C. Ekeke, C. E. Mgbemere, Nwanze, C. N. Aniukwu, F. C, Njoku, C. N. (2025) Musa paradisiaca stem sap extract as corrosion inhibitor for aluminum protection in acidic environment. Zastita Materijala, 66(3),653-664.

[33] A. Kaouka, K. Benarous, M. Keddam (2025) Electrochemical evaluation of natural extracts as effective corrosion inhibitors and surface treatments on metal substrates. Zastita Materijala, 66(3), 483-495.

[34] R. V. Joseph, S. Vimala, D. Amala (2025). Adhutodavasica nees leaf extract as corrosion inhibitor for mild steel in acid medium. Zastita Materijala, 66(2), 429-439.

[35] P. A. Nikolaychuk (2025). Inhibitory Properties of the Boiling Extracts from Fagus Sylvatica Purpurea Fallen Leaves on the Corrosion of Mild Steel in Acidic Environments. Zastita Materijala, 66(1), 206-214.

[36] P. C. Agu,K. Okon (2023)The inhibition of mild steel corrosion by papaya and neem extracts. Zastita materijala, 64(3), 274-282.

[37]T. O. Martins, E. A. Ofudje, A. A. Ogundiran, O. A. Ikeoluwa, O. A. Oluwatobi, E. F. Sodiya, O. Ojo (2022) Cathodic Corrosion Inhibition of Steel by Musa Paradisiaca Leave Extract. Journal of the Nigerian Society of Physical Sciences, 740, Nov. 2022, doi: 10.46481/jnsps.2022.740

[38] H. Sun (1998) COMPASS: An ab Initio Force-Field Optimized for Condensed-Phase Applications Overview with Details on Alkane and Benzene

Compounds. The Journal of Physical Chemistry B, 102(38), 7338–7364, doi: 10.1021/jp980939v

[39] M. McQuaid, H. Sun, D. Rigby(2003)Development and validation of COMPASS force field parameters for molecules with aliphatic azide chains. Journal of Computational Chemistry, vol. 25, no. 1, pp. 61–71, Development and validation of COMPASS force field parameters for molecules with aliphatic azide chains. Journal of Computational Chemistry, 25(1) 61–71, Nov. 2003, doi: 10.1002/jcc.10316.

[40] F. Malaret (2022) Exact calculation of corrosion rates by the weight-loss method. Experimental Results, (3), doi: 10.1017/exp.2022.5

[41] S. Kaya, P. Banerjee, S. kr. Saha, B. Tuzun, C. Kaya (2016) Theoretical evaluation of some benzotriazole and phospono derivatives as aluminum corrosion inhibitors: DFT and molecular dynamics simulation approaches. RSC Advances, 6(78), 74550–74559, doi: 10.1039/c6ra14548e

[42] A. Ahmedal-Amiery, F. F. Sayyid, N. S. Abtan, A. H. Alwazir, H. S. Aljibori, A. M. Mustafa, S. M. Ahmed (2025) Investigation of FPM as a corrosion Inhibitor for mild steel in HCl solution: Insights from electrochemical, weight loss and theoretical approaches. Zastita Materijala, 66(3), 681-693.

[43] I. Lukovits, E. Ka´lma´ n and F. Zucchi (2001) Corrosion Inhibitors—Correlation between Electronic Structure and Efficiency. Corrosion, 57(1), 3–8, doi: 10.5006/1.3290328.

[44] A. Miralrio,A. Espinoza Vázquez (2020) Plant Extracts as Green Corrosion Inhibitors for Different Metal Surfaces and Corrosive Media: A Review. Processes, 8(8)942, Aug. 2020, doi: 10.3390/pr8080942.

[45] O. Dagdag, A. Berisha, Z. Safi, S. Dagdag, M. Berrani, S. Jodeh, C. Verma, E. Ebenso, N. Wazzan,A. Elharfi (2020a) Highly durable macromolecular epoxy resin as anticorrosive coating material for carbon steel in 3% NaCl: Computational supported experimental studies. Journal of Applied Polymer Science,137(34), Jan. 2020, doi: 10.1002/app.49003.

[46] O. Dagdag, L. Guo, Z. Safi, C. Verma, E. E. Ebenso, N. Wazzan, S. Masroor, R. Haldhar, S. Jodeh, M. El Gouri (2020b) Epoxy resin and TiO2 composite as anticorrosive material for carbon steel in 3% NaCl medium: Experimental and computational studies. Journal of Molecular Liquids, (317), 114249, Nov. 2020, doi: 10.1016/j.molliq.2020.114249

[47] O. Dagdag, A. Berisha, Z. Safi, O. Hamed, S. Jodeh, C. Verma, E. Ebenso, A. Elharfi (2019) , DGEBA-polyaminoamide as effective anti-corrosive material for 15CDV6 steel in NaCl medium: Computational and experimental studies. Journal of Applied Polymer Science, (137) doi: 10.1002/app.48402

[48] I. N. Uzochukwu, I. O. Arukalam and N. J. Chigoziri (2023) Anticorrosion performance assessment of silane-modified chitosan/epoxy primer coatings on mild steel in saline environment using computational simulation techniques. Journal of Molecular Modeling, 29(4), doi: 10.1007/s00894-023-05517-4.

[49] C. O .Akalezi, E. E Oguzie (2015) Evaluation of anticorrosion properties of Chrysophyllum albidum leaves extract for mild steel protection in acidic media. International Journal of Industrial Chemistry, 7(1) 81–92, doi: 10.1007/s40090-015-0057-5

IZVOD

EFIKASNOST EKSTRAKTA LISTOVA BILJKE MUSA PARADISIACA (MPL) ZA ZAŠTITU UGLJENIČNOG ČELIKA OD KOROZIJE U MORSKOJ VODI

Efikasnost inhibitora korozije na bazi ekstrakta lista Musa Paradisiaca (MPL) za ugljenični čelik u rastvoru NaCl koncentracije 3,5 tež.% proučavana je korišćenjem Furijeove transformacione infracrvene spektroskopije (FT-IR), gravimetrijske metode (GM), potenciodinamičke polarizacije (PDP) i elektrohemijske impedansne spektroskopije (EIS), merenja kontaktnog ugla (Ö), teorije funkcionalne gustine (DFT) i simulacija molekularne dinamike (MD). FTIR analiza je pokazala prisustvo polarnih funkcionalnih grupa. Dok je GM otkrio efikasnost inhibicije od 91% i smanjenu brzinu korozije sa 0,8817 na 0,0823 mm/god. Slično tome, PDP preko Tafelovih grafikona pokazao je katodni nagib sposoban da kontroliše i reakcije aktivacije (oksidacije) i difuzije (redukcije kiseonika), što ukazuje na inhibitor mešovitog tipa, takođe je koncentracija MPL ekstrakta na 100 g/L pokazala brzinu korozije od oko 0,1 mm/god sa efikasnošću od 90,1%. EIS preko Nikvistovog grafikona pokazao je polukrug sa proširenim prečnikom i povećanim visinama vrhova, što ukazuje na veći otpor prenosa naelektrisanja (Rct). Merenja kontaktnog ugla pokazala su prisustvo tankih filmova na granici metal/inhibitor. Dalje, DFT analiza je pokazala prisustvo centara bogatih elektronima, heteroatoma, polarnih funkcionalnih grupa, što je koreliralo rezultate potvrđujući doprinose izolovanih jedinjenja molekula MPL inhibitora visokoj efikasnosti inhibicije. Pored toga, MD simulacija je pokazala prisustvo Langmirovih filmova na granici inhibitor/metal u ravni orijentaciji i velikoj površinskoj pokrivenosti. Radijalna funkcija raspodele (RDF) pokazala je prisustvo kratkih dužina veza između 2,97 Å-3,49 Å, potvrđujući prisustvo hemijske veze. Ovi istaknuti detalji sugerišu da su performanse inhibicije korozije MPL-a slične onima kod tipičnog surfaktanta i to se pripisuje prisustvu saponina u njegovom molekulu.

Ključne reči: *Korozija ugljeničnog čelika, merenje kontaktnog ugla, DFT i MD simulacija, elektrohemijsko merenje, gravimetrijska analiza, listovi Musa Paradisiaca, surfaktant*

Naučni rad
Rad primljen: 14.09.2025.
Rad korigovan: 13.05.2026.
Rad prihvaćen :14.05.2026.

Osuani F. Idema https://orcid.org/*0000-0001-8710-0052*
Malik Abdulwahab *https://orcid.org/0000-0001-8457-0032*
Innocent O. Arukalam *https://orcid.org/0000-0003-2359-4852*
Ifeyinwa C. Ekeke *https://orcid.org/0000-0002-8165-4449*
Chigoziri N. Njoku *https://orcid.org/0000-0002-8999-3912*
Anyiam N. Chioma *https://orcid.org/0000-0002-8274-3865*
Ikenna B. Onyeachu *https://orcid.org/0000-0003-1090-0611*
Emeka E. Oguzie *https://orcid.org/0000-0003-2708-9298*